Virkkala, V.; Havu, V.; Tuomisto, F.; Puska, M.J.

Origin of band gap bowing in dilute GaAs1-xNx and GaP1-xNx alloys: a real-space view

Published in:
Physical Review B

DOI:
10.1103/PhysRevB.88.035204

Published: 01/07/2013

Document Version
Publisher's PDF, also known as Version of record

Please cite the original version:
Virkkala, V., Havu, V., Tuomisto, F., & Puska, M. J. (2013). Origin of band gap bowing in dilute $GaAs_{1-x}N_x$ and $GaP_{1-x}N_x$ alloys: a real-space view. *Physical Review B*, *88*(3), 1-6. [035204].
https://doi.org/10.1103/PhysRevB.88.035204

Origin of band gap bowing in dilute $GaAs_{1-x}N_x$ and $GaP_{1-x}N_x$ alloys: A real-space view

Ville Virkkala, Ville Havu, Filip Tuomisto, and Martti J. Puska
COMP, Department of Applied Physics, Aalto University, P.O. Box 11100, FI-00076 Aalto, Finland
(Received 15 February 2013; published 16 July 2013)

The origin of the band gap bowing in dilute nitrogen doped gallium based III-V semiconductors is largely debated. In this paper we show the dilute $GaAs_{1-x}N_x$ and $GaP_{1-x}N_x$ as representative examples that the nitrogen-induced states close to the conduction band minimum propagate along the zigzag chains on the {110} planes. Thereby states originating from different N atoms interact with each other resulting in broadening of the nitrogen-induced states which narrows the band gap. Our modeling based on *ab initio* theoretical calculations explains the experimentally observed N concentration dependent band gap narrowing both qualitatively and quantitatively.

DOI: 10.1103/PhysRevB.88.035204 PACS number(s): 71.20.Nr, 61.72.uj, 71.15.Mb

I. INTRODUCTION

Introduction of nitrogen into Ga-based III-V compounds causes a counter-intuitive effect on the band gap, compared to what happens when compound alloys are formed through element mixing on the III sublattice. In the latter case the band gap is given simply by a linear interpolation between the two alloyed compounds. In contrast, the band gap narrows when small fractions of N are added to GaAs, GaP or GaSb,[1–3] although the band gap of GaN, $E_g = 3.30$ eV in zinc blende structure at 0 K,[4] is much wider than that of any of these conventional III-V compounds. This narrowing is not proportional to the fraction of N, and only at sufficiently high N fractions the band gap starts to widen toward that of GaN completing the band gap bowing.

Intriguingly, the band gap narrowing at low N concentration appears to be proportional to the square root of the N content.[1,3,5] In addition, the experimental findings suggest that N incorporation affects both GaAs and GaP in the same way, in spite of the fact that N-induced levels are resonant in the former[6] and in the band gap in the latter.[1] Empirical pseudopotential supercell (SC) calculations[7,8] have not supported simple N-N interactions as the origin of this dependence, while they have been used to explain experimental findings. In particular, it has been stated that the overlap of N impurity wave functions cannot be the origin of these effects, as the extent of the N wave function has been calculated to be only around 6 Å.[7]

While the *ab initio* approaches have not been able to provide an explanation for the observed band bowing, other more phenomenological models have been proposed. The two-level band anticrossing model (BAC)[9] is the most widely applied one. In the BAC model the band gap narrowing results from the interaction of the nitrogen-induced states and the lowest conduction band states of the host material. Tight-binding (TB) methods together with the method where the alloy conduction band edge (CBE) is formed as a linear combination of isolated N states and host material CBE (LCINS method[10,11]) are also used successfully to model the band gap narrowing. Recently, a suggestion has been made, based on *ab initio* SC calculations, that the band gap narrowing is a consequence of the broadening of the nitrogen-induced states caused by N-N interactions.[12] In this model the narrowing in $GaAs_{1-x}N_x$ alloys becomes evident when the N concentration is so large that the broadening of the nitrogen-induced states exceeds the extent of the As $4s$-related bands at the CBE and a new, lower conduction band minimum is formed. However, the actual mechanism for the N-N interactions that causes the broadening of the nitrogen-induced states remains unclear.

In this work we study the formation of the CBE in $GaAs_{1-x}N_x$ and $GaP_{1-x}N_x$ alloys using the density functional theory (DFT) within the local density approximation (LDA). We complement our DFT calculations for periodically repeated SCs by tight-binding (TB) calculations describing the interactions between nitrogen-induced states. Our SC-DFT calculations show that the CBE wave functions of the nitrogen-induced states close to the conduction band minimum (CBM) are of s type around the N atom, but they are also strongly directed along the zigzag chains on the {110} planes. As a result, states originating from quite distant N atoms on common zigzag chains interact and form an effective band that broadens with the increasing N concentration and narrows the band gap. Our TB calculations catch these features and results are in a qualitative and quantitative agreement with experiment.

The paper is organized as follows. Computational methods are described in detail in Sec. II. In Sec. III the calculated band structures and local densities of states (LDOSs) are shown and analyzed in detail. The developed TB model based on DFT results is introduced and the results calculated by this model are compared to both experimental and DFT results. Section IV is a summary and in the appendix the developed TB method is described in detail.

II. METHODS

All our DFT calculations are performed within LDA using the VASP code,[13] with the projector augmented wave method.[14] The LDA approximation enables the use of large supercells and it describes qualitatively but also quantitatively correctly the nitrogen-induced changes in the conduction band states, compared to hybrid functionals that give band gaps more close to experimental ones.[15] The valence electron configurations, used in calculations, for Ga, As, P, and N are $4s^2 4p^1$, $4s^2 4p^3$, $3s^2 3p^3$, and $2s^2 2p^3$, respectively. According to our test calculations including the Ga $3d$ electrons as the valence in the case of a single N atom in the 64-atom SC, treating the Ga $3d$ electrons as core gives qualitatively and also quantitatively

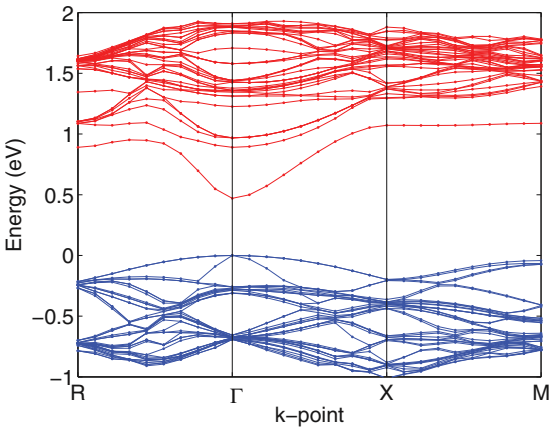

FIG. 1. (Color online) Band structure of the periodic $Ga_{256}As_{255}N$ system. The energy zero coincides with the top of the valence band. The vertical lines are a guide to an eye and indicate the positions of the high-symmetry points.

good descriptions of the band structures in $GaAs_{1-x}N_x$ and $GaP_{1-x}N_x$ alloys. A cutoff energy of 400 eV is used for the plane-wave basis set, which provides a good convergence of the total energy. A 2×2×2 Monkhorst-Pack set is used for the **k**-point sampling in structural optimization and total energy optimization in band structure calculations. The densities of states (DOS) are generated using a 3×3×3 Monkhorst-Pack set for the **k**-point sampling and the Brillouin zone integration is performed using a linear tetrahedron method in DOS calculations. The stopping criterion for ionic relaxation is that the forces acting on each atom are smaller than 0.02 eV/Å. The lattice constants are optimized for different sizes of supercells containing N atoms. We study cubic $GaAs_{1-x}N_x$ and $GaP_{1-x}N_x$ SC's containing from 64 up to 512 atoms with one or two substitutional N atoms.

To model more realistic structures we developed a TB model to complement our DFT calculations, that takes only into account the interactions between the N atoms. We are thereby able to treat systems of tens of thousands of N atoms randomly distributed between the anion sites of the host lattice. The TB model developed is described in detail in the appendix.

III. RESULTS

SC-DFT calculations model alloys through band structures corresponding to the superlattice periodicity. Although this is an artificial approach for a random alloy it gives valuable first-principles information about the N-host and N-N interactions. Figure 1 shows the band structure of the periodic $Ga_{256}As_{255}N$ system in the small first Brillouin zone corresponding to the large unit cell of 512 atoms. The lowest conduction band, i.e., the CBE is flat outside the central region and bends down when approaching the Γ point. The flat region is due to the localized nitrogen-induced resonant states that hybridizes especially near the Γ point with GaAs bulk states. Anticipating our discussion below the strong dispersion near the Γ point can also be interpreted to originate from long-range nitrogen-induced resonant states interacting with each other.

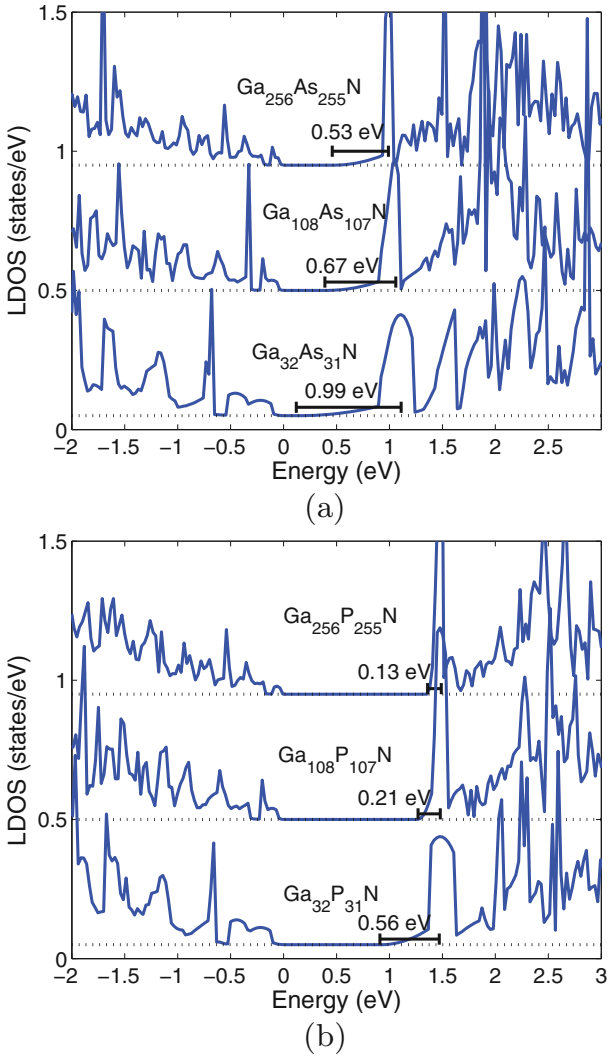

FIG. 2. (Color online) First-principles LDOSs at an N atom in $GaAs_{1-x}N_x$ and $GaP_{1-x}N_x$ supercells. The solid horizontal segments indicate the distance between the peak maxima, related to the dispersionless nitrogen-induced band outside the center of the first Brillouin zone (see Fig. 1), and the conduction band minimum. The energy zero coincides with the top of the valence band.

The nitrogen-induced states result in characteristic features in the LDOS's. Figure 2(a) shows the LDOSs for $Ga_{256}As_{255}N$, $Ga_{108}As_{106}N$, and $Ga_{32}As_{31}N$ systems. LDOSs have a narrow peak and a low intensity tail toward lower energies corresponding to the flat and dispersive regions of the CBE (see Fig. 1), respectively. We find these features also in the case of $GaP_{1-x}N_x$ as is evident in Fig. 2(b) for $Ga_{256}P_{255}N$, $Ga_{108}P_{107}N$, and $Ga_{32}P_{31}N$ systems. In comparison with GaAs host the LDOS peak related to nitrogen-induced states in GaP is at the same N concentrations lower in energy with respect to the CBM and the extent of the LDOS tail is clearly smaller. When the size of the SC is reduced from 512 to 216 and further to 64 atoms the peak corresponding to nitrogen-induced states broadens in both alloys but stays stationary with respect to the top of the valence band and the LDOS tail reaches deeper into the band gap causing its reduction. This behavior is in a good qualitative agreement with the behavior of the A

TABLE I. Band gap reductions and LDOS tail lengths (see Fig. 2) for different periodic $GaAs_{1-x}N_x$ and $GaP_{1-x}N_x$ systems. The band gap reduction is determined at the Γ point of the superlattice.

System SC	ΔE_g (eV)	Tail length (eV)
$Ga_{256}As_{255}N$	0.02	0.53
$Ga_{108}As_{107}N$	0.09	0.67
$Ga_{32}As_{31}N$	0.34	0.99
$Ga_{256}P_{255}N$	0.13	0.13
$Ga_{108}P_{107}N$	0.22	0.21
$Ga_{32}P_{31}N$	0.57	0.56

line in photoluminescence spectra for $GaP_{1-x}N_x$ alloys with increasing N concentration.[1]

The reduction of the band gap and the length of the LDOS tail below the peak corresponding to nitrogen-induced states for the GaAs and GaP SCs with a single N atom and of different sizes are given in Table I. For GaP the band gap reduction is in practice the same as the length of the LDOS tail reflecting the position of the nitrogen-induced states just at the bulk CBM at the Γ point. In the case of GaAs a bias of about 0.5–0.6 eV should be subtracted from the length of the LDOS tail to obtain the band gap reduction. The bias is due to the location of the peak corresponding to nitrogen-induced resonant states within the bulk conduction band. The lengthening of the LDOS tail causing the band gap reduction is a common feature for the $GaAs_{1-x}N_x$ and $GaP_{1-x}N_x$ systems calling for a uniform picture for these materials.

Figure 3 shows the CBE partial charge density in GaAs around an N atom as a density isosurface. In GaP we find a similar behavior. The partial charge density is obtained by summing the densities from all the **k**-points used in the calculation. The SC used contains 512 atoms and the isosurface is viewed along a ⟨111⟩ direction so that a Ga atom is on top of the N atom in the center of the figure. The density

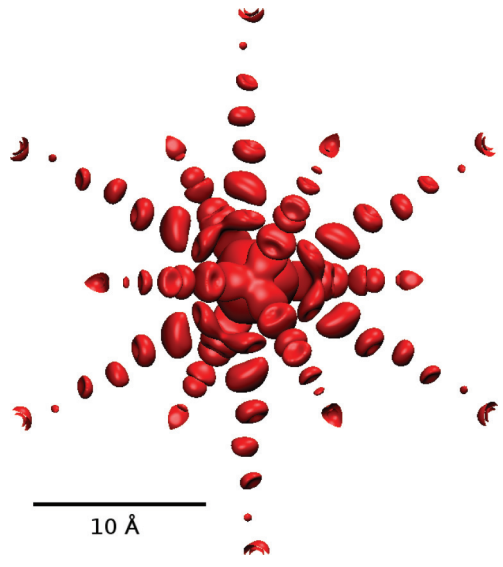

FIG. 3. (Color online) CBE partial charge density in the $Ga_{256}As_{255}N$ SC, viewed along the ⟨111⟩ direction. The isosurface shown corresponds to a density isovalue of 0.0012. The N atom is located at the center of the figure.

TABLE II. Band gap reduction due to a single N atom or two N atoms in the 512- and 216-atom GaAs SCs. Three different configurations are considered for two N atoms.

Configuration	ΔE_g (eV)
$Ga_{256}As_{255}N$	0.02
$Ga_{256}As_{254}N_2$ [(1,1,0)a]	0.09
$Ga_{256}As_{254}N_2$ [(1,1,1)a]	0.06
$Ga_{256}As_{254}N_2$ [(1,0,0)a]	0.04
$Ga_{108}As_{107}N$	0.09
$Ga_{108}As_{106}N_2$ [(1,1,0)a]	0.20
$Ga_{108}As_{106}N_2$ [(1,1,1)a]	0.17
$Ga_{108}As_{106}N_2$ [(1,0,0)a]	0.12
$Ga_{32}As_{31}N$	0.34

agglomerates strongly around the N atom and stretches out toward the four nearest-neighbor Ga atoms and the N-Ga back bonds. Thereafter, the agglomeration of the CBE partial charge density is directed toward the 12 zigzag directions (six of them are on a {111} plane perpendicular to the direction of view, three of them point upwards and three downwards from that {111} plane). We have checked that the CBE partial density from all the **k**-points, including those with dispersion and near the Γ point, have this anisotropic character. The interaction between the nitrogen-induced states takes place along the the zigzag chains with the CBE partial charge agglomeration. Thus, when the N concentration increases both the width of the narrow LDOS peak and the extent of the LDOS tail increase simultaneously with the strengthening of the CBE partial charge agglomeration on the connecting zigzag chains.

The tendency of the CBE charge to localize along the zigzag chains is strongly connected with ionic relaxations, initiated by the strong and short Ga-N bonds also propagating along these chains. According to our SC-DFT calculations the Ga-N bond attains in GaAs and GaP nearly the same value as in bulk GaN resulting in an inward relaxation of the nearest neighbor Ga atoms by 13%–16% of the bond length of the GaAs and GaP lattices. A similar strong ionic relaxation along the zigzag directions has been previously observed in the case of the vacancy in silicon[16] and a similar anisotropy of localized N derived states in GaAs and GaP was predicted by Kent and Zunger.[7] We can see the agglomeration of the CBE partial charge density also when we omit the ionic relaxation from ideal lattice positions but then the effect is clearly weaker and shorter in range. This is in agreement with Kent and Zunger[7] who predicted a stronger band gap reduction when the ionic structures were relaxed in SC calculations.

We have studied the anisotropy and strength of the N-N interaction also by inserting two N atoms at different positions in GaAs SC's of 216 and 512 atoms. The studied representative configurations contain one N atom in the origin and another one in the (1,1,1)a, (1,1,0)a, or (1,0,0)a location, where a is the lattice parameter of the conventional unit cell. The results are given in Table II in terms of the reduction of the band gap with respect to the GaAs bulk band gap. The behavior of the band gap is qualitatively similar for the two SC sizes signalizing from the interaction between the N atoms inside the same SC. The strongest reduction in the band gap is observed for the (1,1,0)a configuration in accordance with the above discussion

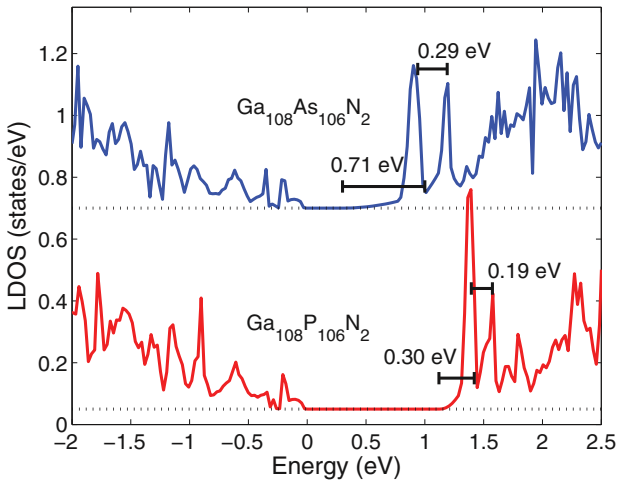

FIG. 4. (Color online) First-principles LDOSs corresponding to two N atoms at neighboring anion sites in $Ga_{108}As_{106}N_2$ and $Ga_{108}P_{106}N_2$ systems. The solid segments indicate the distance between the two peaks related to nitrogen-induced states and the distance between the center of mass of the two peaks and the minimum eigenvalue. The energy zero coincides with the top of the valence band.

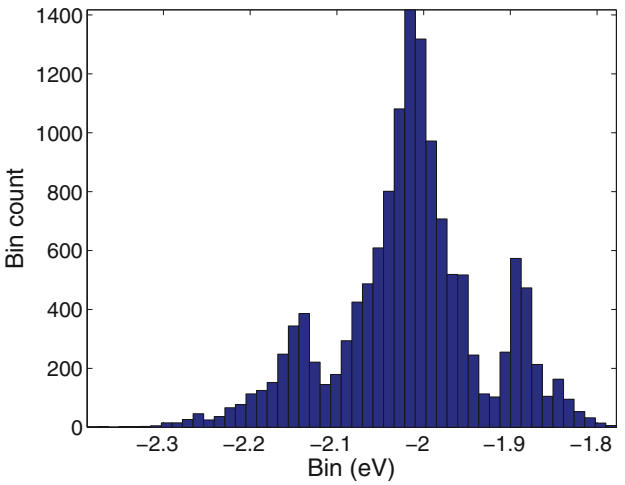

FIG. 5. (Color online) TB eigenvalue distribution corresponding to a random sample of 13 824 N atoms (3.1% concentration) in the $GaAs_{1-x}N_x$ alloy.

about the anisotropy of the nitrogen-induced resonant states. In the (1,0,0)*a* configuration the N atoms are not along the same zigzag chain and consistently the band gap reduction is modest compared to the case of a single N atom in the SC. In the (1,1,1)*a* configuration the band gap reduction is intermediate between those of the (1,1,0)*a* and (1,0,0)*a* configurations. This is due to the fact that the strong back bond at a Ga atom caused by one of the N atoms is next to the other N atom.

In order to study the effect of the interactions between the nitrogen-induced states on the band gap reduction in random structures in accordance with the experimental conditions we have developed on the basis of our *ab initio* results a TB model, in which only interactions between N atom sites connected through zigzag chains are included. In our model the nondiagonal matrix elements $h_{i,j}$, describing the interaction between the N atom sites i and j, are defined as $h_{i,j} = k/r_{i,j}^{\alpha}$ if the sites are connected through a zigzag chain and $h_{i,j} = 0$ otherwise. Here $r_{i,j}$ is the distance between the two N atoms. The power-law decay reflects the long-range tendency of the directional interaction. The diagonal terms $h_{i,i}$ are set to a constant value describing the energy level of the nitrogen-induced states. To determine the parameters k and α we used our LDOS results calculated within the SC-DFT scheme for four large structures of a single N atom in the SCs of 64, 216, 512 atoms (Fig. 2) and of two N atoms at the nearest anion sites in the 216-atom SC (Fig. 4). The parameter values of $k = -0.67$ eVÅ$^{\alpha}$, $\alpha = 1.28$ reproduce the DFT LDOS peak and tail structures (see Fig. 2) of N in GaAs and $k = -0.59$ eVÅ$^{\alpha}$, $\alpha = 1.43$ those of N in GaP. The implementation of the developed method is explained in more detail in the appendix.

Using our *ab initio*–based TB model we study changes in the CBE as a function of the N concentration. We randomly distribute from 384 up to 13 824 N atoms into a SC of 442 368 anion sites. The resulting Hamiltonian matrix is diagonalized and a broadened eigenvalue distribution around the original energy level of nitrogen-induced states is obtained. Between the extreme values there exists a distribution of eigenvalues corresponding to the continuous broadening of the nitrogen-induced states seen in the LDOSs. Figure 5 shows as an example the distribution for a large $GaAs_{1-x}N_x$ sample with an N concentration of 3.1%. The highest peak is due to the isolated N atoms and the two lower ones are related to N-N pairs. These features are in agreement with the measured scanning tunneling spectra.[6]

We plot, respectively, in Figs. 6(a) and 6(b) for $GaAs_{1-x}N_x$ and $GaP_{1-x}N_x$ for each N concentration the minimum and maximum values of the eigenvalue distribution. The values are averaged over 100 different random samples. The extreme values show a square-root-like behavior, which is, in the case $GaAs_{1-x}N_x$, in a good agreement with photomodulated reflectance measurements for the N-induced band gap reduction and an N-induced feature in the conduction band.[5] Similarly, for $GaP_{1-x}N_x$ our results are in good agreement with the band gap reduction measured by photoluminescence[1] and photomodulated transmission spectroscopy.[17] Our present SC-DFT results shown in Fig. 4 as well as earlier SC-DFT calculations[7,15] give a linear dependence of the band gap reduction on the N concentration which is in a clear disagreement with experimental findings. The reason for the linear dependence is the fact that N atoms of the neighboring SCs are on the same zigzag chains resulting in a surplus of N-N interactions with relatively short distances in comparison with the random N atom distribution of the same concentration.

IV. CONCLUSIONS

In this work we demonstrated using *ab initio* calculations how the nitrogen-induced states near the CBM propagate along zigzag chains in $GaAs_{1-x}N_x$ and $GaP_{1-x}N_x$ alloys. This results in coupling between states originating from different N atoms which becomes stronger with increasing N concentration leading to the broadening of the distribution of nitrogen-induced states. On the basis of our DFT results

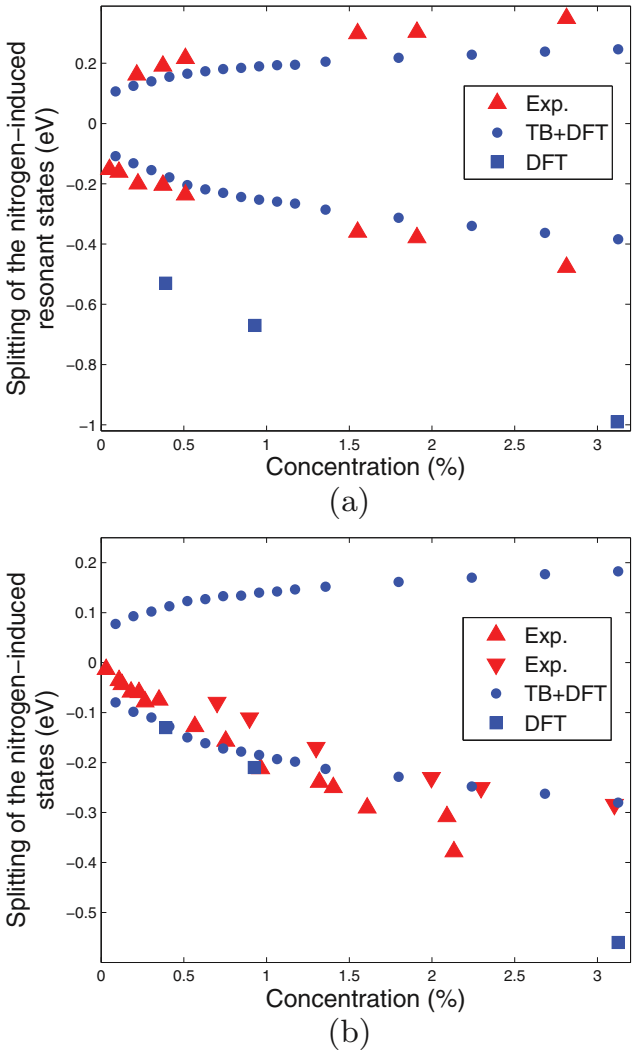

FIG. 6. (Color online) Broadening of the distribution of nitrogen-induced states as a function of N concentration in (a) $GaAs_{1-x}N_x$ and (b) $GaP_{1-x}N_x$. Blue circles and squares give our random-system TB and SC-DFT results, respectively. For $GaAs_{1-x}N_x$ red triangles are experimental data from Ref. 5 (measurement temperature 300 K), whereas for $GaP_{1-x}N_x$ red upright and downright triangles are experimental data from Refs. 1 (20 K) and 17 (room temperature), respectively. The energy zero is the energy level corresponding to isolated nitrogen-induced states (in calculations the position of the peak corresponding to nitrogen-induced states in LDOS). To align the experimental and calculated energy levels corresponding to nitrogen-induced states in $GaAs_{1-x}N_x$ the experimental data is shifted to locate symmetrically with respect to the energy zero.

we constructed a TB model for the interaction of the nitrogen-induced states and applied it in large random systems of N atoms in GaAs and GaP. The model predicts a square-root-like broadening of the distributions of nitrogen-induced states as a function of the N concentration and a corresponding narrowing of the band gap in agreement with experiments. The square-root-like behavior is due to the interplay between the directional and long-range characters of the interactions between the nitrogen-induced states. Thus, the band gap narrowing in dilute III-V nitrides can be qualitatively and quantitatively explained by *ab initio* calculations, and it is an inherent property of the interactions between nitrogen-induced states mediated by the host lattice, rather than nitrogen host material CBE interaction.

ACKNOWLEDGMENTS

We acknowledge the Suomen Kulttuurirahasto foundation for financial support. This work has been supported by the Academy of Finland through the Center of Excellence program. The computer time was provided by CSC – the Finnish IT Center for Science.

APPENDIX: DEVELOPED TB MODEL

We have developed a TB model describing the interaction between nitrogen-induced states originating from N atoms substituting anions in a III-V compound semiconductors. The nondiagonal matrix elements $h_{i,j}$ corresponding to the N atoms i and j, are defined as $h_{i,j} = k/r_{i,j}^{\alpha}$ if atoms i and j, separated by the distance $r_{i,j}$, are connected trough a zigzag chain and $h_{i,j} = 0$ otherwise. The diagonal terms are set to an arbitrary chosen constant value E_{s^*} describing the energy level of the isolated nitrogen-induced states. The units are electron volts and angstroms. Using the supercell approximation with periodic boundary conditions and the Γ-point approximation the nonzero matrix elements $h_{i,j}$ become

$$h_{i,j} = \sum_{\mathbf{L}} \frac{k}{|\hat{\mathbf{r}}_{i,j} + \mathbf{L}|^{\alpha}}, \tag{A1}$$

where $\mathbf{L}$ is a vector of the superlattice. The restriction on the interactions to the zigzag chains and the use of simple-cubic supercells modifies Eq. (A1) to the form,

$$h_{i,j} = \sum_{\phi} \sum_{n=0}^{\infty} \frac{k}{(r_{i,j_\phi} + \sqrt{2}nL)^{\alpha}}, \tag{A2}$$

where ϕ runs over all directions where the N atoms i and j are connected through a zigzag chain and L is the side length of the cubic supercell. The diagonal terms become

$$h_{i,i} = E_{s^*} + 12 \sum_{n=1}^{\infty} \frac{k}{(\sqrt{2}nL)^{\alpha}}. \tag{A3}$$

The inner sum in Eq. (A2) is the Hurwitz zeta function and it can be evaluated efficiently using the Euler-Maclaurin summation formula.[18]

To determine the free parameters k and α, we created large ordered structures corresponding to single N atom in 64-, 216-, 512-atoms supercells and two N atoms at the neighboring anion sites in the 216-atom supercell and fitted the parameters k and α so that the TB eigenvalue distribution reproduces the characteristic features in our first-principles LDOS results shown in Figs. 2(a), 2(b), and 4. In the case of a single N atom the fitted feature is the tail length and in the case of two N atoms the fitted features are both the distance between the peaks corresponding to the bonding and antibonding wave functions and the distance between their center of mass and the conduction band minimum. The optimal k and α are found by searching for each value of α the optimal k value in the least squares sense. The obtained parameters are

$k = -0.67$ eVÅ$^{\alpha}$, $\alpha = 1.28$ ($GaAs_{1-x}N_x$) and $k = -0.59$ eVÅ$^{\alpha}$, $\alpha = 1.43$ ($GaP_{1-x}N_x$).

In the case of GaAs we checked the possibility that the N-N interactions are not restricted to the zigzag chains and modeled them using the short-range exponential decay. However, this model does not reproduce the DFT results in Figs. 2(a), 2(b), and 4 and the error in the fit becomes nearly four times larger than in the case where the interaction are restricted on the zig-zag chains.

To simulate real structures, we distributed randomly from 384 up to 13 824 N atoms into a supercell of 442 368 anion sites. The resulting Hamiltonian matrix is diagonalized and a broadened eigenvalue distribution around the original energy level of nitrogen-induced states is obtained. Figure 5 shows the obtained distribution in the case of 13 824 N atoms. The side peaks around the nitrogen-induced peak results from the N pairs located at the neighboring anion sites.

[1] H. Yaguchi, S. Miyoshi, G. Biwa, M. Kibune, K. Onabe, Y. Shiraki, and R. Ito, J. Cryst. Growth **170**, 353 (1997).

[2] Y. Zhang, A. Mascarenhas, J. F. Geisz, H. P. Xin, and C. W. Tu, Phys. Rev. B **63**, 085205 (2001).

[3] T. D. Veal, L. F. J. Piper, S. Jollands, B. R. Bennett, P. H. Jefferson, P. A. Thomas, C. F. McConville, B. N. Murdin, L. Buckle, G. W. Smith, and T. Ashley, Appl. Phys. Lett. **87**, 132101 (2005).

[4] I. Vurgaftman, J. R. Meyer, and L. R. Ram-Mohan, J. Appl. Phys. **89**, 5815 (2001).

[5] P. J. Klar, H. Grüning, W. Heimbrodt, J. Koch, F. Höhnsdorf, W. Stolz, P. M. A. Vicente, and J. Camassel, Appl. Phys. Lett. **76**, 3439 (2000).

[6] L. Ivanova, H. Eisele, M. P. Vaughan, Ph. Ebert, A. Lenz, R. Timm, O. Schumann, L. Geelhaar, M. Dähne, S. Fahy, H. Riechert, and E. P. O'Reilly, Phys. Rev. B **82**, 161201 (2010).

[7] P. R. C. Kent and A. Zunger, Phys. Rev. B **64**, 115208 (2001).

[8] T. Mattila, S.-H. Wei, and A. Zunger, Phys. Rev. B **60**, R11245 (1999).

[9] W. Shan, W. Walukiewicz, J. W. Ager III, E. E. Haller, J. F. Geisz, D. J. Friedman, J. M. Olson, and S. R. Kurtz, Phys. Rev. Lett. **82**, 1221 (1999).

[10] C. Harris, A. Lindsay, and E. P. O'Reilly, J. Phys.: Condens. Matter **20**, 295211 (2008).

[11] A. Lindsay and E. P. O'Reilly, Phys. Rev. Lett. **93**, 196402 (2004).

[12] H.-X. Deng, J. Li, S.-S. Li, H. Peng, J.-B. Xia, L.-W. Wang, and S.-H. Wei, Phys. Rev. B **82**, 193204 (2010).

[13] G. Kresse and J. Furthmüller, Comput. Mater. Sci. **6**, 15 (1996).

[14] G. Kresse and D. Joubert, Phys. Rev. B **59**, 1758 (1999).

[15] V. Virkkala, V. Havu, F. Tuomisto, and M. J. Puska, Phys. Rev. B **85**, 085134 (2012).

[16] C. Z. Wang, C. T. Chan, and K. M. Ho, Phys. Rev. Lett. **66**, 189 (1991).

[17] W. Shan, W. Walukiewicz, K. M. Yu, J. Wu, J. W. Ager III, E. E. Haller, H. P. Xin, and C. W. Tu, Appl. Phys. Lett. **76**, 3251 (2000).

[18] W. H. Press, S. A. Teukolsky, W. T. Vetterling, and B. P. Flannery, *Numerical Recipes: the Art of Scientific Computing*, 3rd ed. (Cambridge University Press, New York, 2007).